

Nonradial superfluid modes in oscillating neutron stars

A. I. Chugunov^{*}, M. E. Gusakov[†]

Ioffe Physical-Technical Institute of the Russian Academy of Sciences, Politekhnicheskaya 26, 194021 Saint-Petersburg, Russia

Accepted 2011 xxxx. Received 2011 xxxx; in original form 2011 xxxx

ABSTRACT

For the first time nonradial oscillations of superfluid nonrotating stars are self-consistently studied at finite stellar temperatures. We apply a realistic equation of state and realistic density dependent model of critical temperature of neutron and proton superfluidity. In particular, we discuss three-layer configurations of a star with no neutron superfluidity at the centre and in the outer region of the core but with superfluid intermediate region. We show, that oscillation spectra contain a set of modes whose frequencies can be very sensitive to temperature variations. Fast temporal evolution of the pulsation spectrum in the course of neutron star cooling is also analysed.

Key words: stars: neutron – stars: oscillations – stars: interiors.

1 INTRODUCTION

Studying the pulsations of neutron stars (NSs) is very important and actively developing area of research, since comparison of pulsation theory with observations can potentially give valuable information about the properties of superdense matter (Andersson et al. 2011). Yet, it is an extremely difficult theoretical problem even for normal (nonsuperfluid) stars. Superfluidity of baryons additionally complicates the theory because in superfluid (SFL) matter one should deal with several independent velocity fields. As a consequence, the hydrodynamics describing pulsations of SFL NSs is much more complicated in comparison to ordinary (normal) hydrodynamics (e.g., Gusakov 2007).

In this letter we report on a substantial progress in modeling and understanding the nonradial oscillations of nonrotating SFL NSs in full general relativity. It should be noted that the nonradial oscillations of such stars have been intensively studied in the literature starting from the seminal paper by Lindblom & Mendell (1994). In particular, nonradial oscillations of general relativistic NSs were considered by Comer, Langlois & Lin (1999); Andersson, Comer, & Langlois (2002); Yoshida & Lee (2003); Lin, Andersson & Comer (2008). Because of the complexity of the problem, most of these papers used a simplified microphysics input, i.e., toy-model equations of state and simplified models of baryon superfluidity (see, however, Lin et al. 2008; Haskell, Andersson & Passamonti 2009; Haskell & Andersson 2010). Moreover, in *all* these studies SFL matter was treated as being at zero temperature, an assumption that is unjustified at not too low stellar temperatures and may lead to a quantitatively

incorrect oscillation spectra (Gusakov & Andersson 2006; Kantor & Gusakov 2011; this letter).

Here we improve on this by considering nonradial oscillations of SFL neutron stars at *finite* temperatures. We follow an approach of Gusakov & Kantor (2011) (hereafter GK11) which allows us to analyse oscillations of general relativistic NSs employing realistic equation of state, density dependent profiles of nucleon critical temperatures and fully relativistic finite-temperature SFL hydrodynamics.

As it was first found by Lindblom & Mendell (1994), oscillation spectrum of a SFL NS consists of two distinct classes of modes, the so called normal and superfluid modes. The frequencies of normal modes almost coincide with the oscillation frequencies of a normal star and hence are independent of temperature. The spectrum of these modes is therefore very well studied in the literature (see, e.g., Thorne & Campolattaro 1967; McDermott, Van Horn & Hansen 1988; Benhar, Ferrari & Gualtieri 2004). On the contrary, SFL modes can be very temperature-dependent. Using the approach of GK11 they can be decoupled from the normal modes and studied separately. Since radial SFL modes have already been thoroughly analysed in Kantor & Gusakov (2011), here we focus on the nonradial SFL modes. In what follows, the speed of light $c = 1$.

2 BASIC EQUATIONS

In this section we briefly discuss the equation describing SFL oscillation modes [Eq. (5)]. The detailed derivation of this equation can be found in GK11. We consider a NS with nucleonic core and assume that both neutrons (n) and protons (p) can be superfluid. Following GK11, we introduce the baryon current density $j_{(b)}^\mu = j_{(n)}^\mu + j_{(p)}^\mu$, where

^{*} andr.astro@mail.ioffe.ru

[†] gusakov@astro.ioffe.ru

$$j_{(i)}^\mu = n_i u^\mu + Y_{ik} w_{(k)}^\mu \quad (1)$$

is the current density for particles $i = n$ or p (e.g., Kantor & Gusakov 2011). Here and below the summation is assumed over the repeated nucleon index $k = n, p$. In Eq. (1) n_i is the number density; w^μ is the four-velocity of “normal” liquid component; $w_{(k)}^\mu$ is the four-vector that characterizes motion of superfluid neutron ($k = n$) or proton ($k = p$) component with respect to normal matter. Finally, the symmetric temperature-dependent matrix Y_{ik} ($= Y_{ki}$) is a relativistic analogue of the SFL entrainment matrix. Since electrons (e) are normal, their current density is $j_{(e)}^\mu = n_e u^\mu$, where n_e is the electron number density. The quasineutrality implies $n_e = n_p$ (for simplicity, we ignore possible admixture of muons in the core).

In this letter we study small-amplitude (linear) oscillations of a *nonrotating* star being initially in hydrostatic equilibrium. Hence, for the unperturbed star one has $u^\mu = (e^{-\nu/2}, 0, 0, 0)$ and $w_{(n)}^\mu = w_{(p)}^\mu = 0$, while the metric is $dS^2 = -e^\nu dt^2 + e^\lambda dr^2 + r^2 d\Omega^2$, where r and t are the radial and time coordinates, respectively; $\nu(r)$ and $\lambda(r)$ are the metric functions; and Ω is the solid angle in a spherical frame with the origin at the stellar centre. For definiteness, we assume that the unperturbed matter in the stellar core was in beta-equilibrium, $\delta\mu \equiv \mu_n - \mu_p - \mu_e = 0$, where μ_d is the chemical potential for particles $d = n, p, e$. We also restrict ourselves to oscillations with vanishing electrical current, $j_{(p)}^\mu - j_{(e)}^\mu = 0$. The latter condition couples the SFL degrees of freedom,

$$w_{(p)}^\mu = -(Y_{pn}/Y_{pp}) w_{(n)}^\mu. \quad (2)$$

As it was shown in GK11 the interaction between the SFL and normal oscillation modes is controlled by the coupling parameter s , which is given by $s = (n_e \partial P / \partial n_e) / (n_b \partial P / \partial n_b)$ where $P(n_b, n_e)$ is the pressure and $n_b = n_n + n_p$ is the baryon number density. This parameter is small for a wide set of realistic equations of state, $|s| \lesssim 0.05$ (see fig. 1 in GK11), so that the approximation of completely decoupled SFL and normal modes ($s = 0$) is already sufficient to calculate the pulsation spectrum within an accuracy of a few per cent. In the $s = 0$ approximation the quantities $j_{(b)}^\mu$, P , and the metric $g_{\mu\nu}$ remain unperturbed for SFL oscillation modes. This opens up a possibility to formulate an equation describing SFL modes that depends *only* on SFL degrees of freedom, i.e., on $w_{(k)}^\mu$. This equation follows from the energy-momentum conservation and potentiality condition for motion of SFL neutrons. For a nonrotating star it takes the form (see GK11)

$$\omega (\mu_n Y_{nk} w_{(k)j} - n_b w_{(n)j}) = n_e \partial_j (\delta\mu^\infty), \quad (3)$$

where $\delta\mu^\infty \equiv \delta\mu e^{\nu/2}$ and the disbalance $\delta\mu(n_b, n_e)$ equals

$$\delta\mu = -\iota e^{\nu/2} \frac{\mathfrak{B} n_e}{\omega} \left[\frac{Y_{nk}}{n_e n_b} \frac{\partial n_e}{\partial x^\mu} w_{(k)}^\mu + \left(\frac{Y_{nk}}{n_b} w_{(k)}^\mu \right)_{;\mu} \right]. \quad (4)$$

In Eqs. (3) and (4) $j = 1, 2, \text{ or } 3$ is the space index, $\partial_j \equiv \partial / (\partial x^j)$, $\mathfrak{B} \equiv \partial \delta\mu(n_b, n_e) / \partial n_e$, and all perturbations are assumed to be $\propto \exp(\omega t)$. Because Eq. (3) is linear, one can generally present $\delta\mu^\infty$ as: $\delta\mu^\infty(r, \Omega) = \delta\mu_l(r) Y_{lm}(\Omega)$, where $Y_{lm}(\Omega)$ is the spherical harmonic [notice that $\delta\mu_l(r)$ does not depend on the index m , see Eq. (5)]. Combining

then Eqs. (2), (3), and (4) one obtains the following equation

$$0 = \delta\mu_l'' + \left(\frac{h'}{h} - \frac{\lambda'}{2} + \frac{2}{r} \right) \delta\mu_l' - e^\lambda \left[\frac{l(l+1)}{r^2} + e^{-\nu/2} \frac{\omega^2}{h \mathfrak{B}} \right] \delta\mu_l. \quad (5)$$

Here prime means derivative with respect to r and $h = e^{\nu/2} n_e^2 / (\mu_n n_b y)$, where $y = n_b Y_{pp} / [\mu_n (Y_{nn} Y_{pp} - Y_{np}^2)] - 1$.

Eq. (5) determines the eigenfrequencies of SFL oscillation modes and is valid in the region of the stellar core where neutrons are superfluid (hereafter, SFL-region). This equation depends on the internal stellar temperature T only through the parameter $y = y(T/T_{cn}, T/T_{cp})$, where $T_{ci}(r)$ is the profile of critical temperatures for particles $i = n$ or p . The boundary conditions to Eq. (5) are following. If neutrons in the stellar centre are superfluid, the regularity of the solution requires $\delta\mu_l \propto r^l$ at $r \rightarrow 0$. If the outer boundary of the SFL-region coincides with the crust-core interface (where $r = R_{cc}$), then the SFL current should not penetrate the crust. This condition implies $\delta\mu_l'(R_{cc}) = 0$. Finally, if T is so high, that the SFL-region does not spread all over the core, then its boundaries are determined by the condition $T = T_{cn}(r)$ (see Sec. 3 for more details). In that case, the regularity of the solution at such boundaries requires $\delta\mu_l' = e^{\lambda-\nu/2} \omega^2 \delta\mu_l / (h' \mathfrak{B})$.

Thus, we reduce the problem of calculation of SFL modes to solving simple second-order differential Eq. (5). For any fixed multipolarity l the solution to Eq. (5) consists of a set of eigenfrequencies ω_{ln} and eigenfunctions $\delta\mu_{ln}(r)$ which differ by the number of radial nodes $n = 0, 1, 2, \dots$

3 MICROPHYSICS INPUT AND NS MODEL

Prior to studying the SFL oscillations using Eq. (5), one has to specify equation of state (including profiles of T_{cn} and T_{cp}) and construct a hydrostatic model of an unperturbed star. In addition, one has to specify the profile of internal stellar temperature. High thermal conductivity leads to a rapid equilibration of T in the NS core (see, e.g., Gnedin, Yakovlev & Potekhin 2001). As a result, the red-shifted internal temperature $T^\infty = T e^{\nu/2}$ becomes almost constant. Moreover, as it was shown by Gusakov & Andersson (2006), for the SFL-region to be in hydrostatic and beta-equilibrium it must be in thermal equilibrium. Thus, in what follows we assume that $T^\infty = \text{const}$ in the SFL-region.

In the present letter we employ the equation of state suggested by Akmal, Pandharipande & Ravenhall (1998) (APR). The coupling parameter s for such an equation of state is small, $|s| \sim 0.02$. The density profiles of T_{cn} and T_{cp} that we use here are shown in the left panel of Fig. 1. They do not contradict to results of microscopic calculations (see, e.g., Lombardo & Schulze 2001) and are similar to the nucleon pairing models used to explain observations of the cooling NS in Cas A supernova remnant (Shternin et al. 2011). For definiteness, all calculations are performed for a star of the mass $1.4 M_\odot$ and circumferential radius $R = 12.2$ km.

Since T^∞ , but not T , is constant in the SFL-region, it is convenient to introduce the *red-shifted* nucleon critical temperatures $T_{ck}^\infty \equiv e^{\nu/2} T_{ck}$ ($k = n, p$) to analyse how the size of SFL-region changes with T^∞ . The functions $T_{cn}^\infty(r)$ and

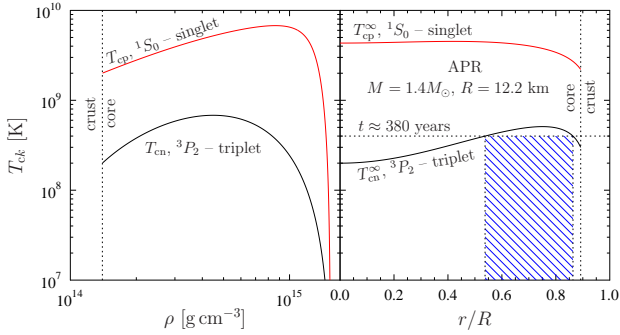


Figure 1. (color online) Left panel: Nucleon critical temperatures T_{ck} versus density ρ ($k = n, p$). Right panel: Red-shifted critical temperatures T_{ck}^{∞} versus radial coordinate r .

$T_{cp}^{\infty}(r)$ are shown on the right panel of Fig. 1. The red-shifted proton critical temperature is high, $T_{cp}^{\infty}(r) \sim 2 \times 10^9$ K, so that superfluid protons occupy the entire core almost immediately after the NS birth. The function $T_{cn}^{\infty}(r)$ has a maximum $\mathfrak{T}_{cn}^{\infty} \approx 5.1 \times 10^8$ K at $r = r_{cn}^{\max} \approx 0.75R$. Near the stellar centre the density varies slowly with r which results in a weak dependence of T_{cn}^{∞} on the radial coordinate. As the star cools down to $T^{\infty} \lesssim \mathfrak{T}_{cn}^{\infty}$, the SFL-region is formed, initially, as a narrow spherical layer. Upon subsequent cooling the layer becomes wider and, for example, at $T^{\infty} = 4 \times 10^8$ K it is shown by the hatched region in the figure. As the temperature decreases further, the SFL-region extends to the crust and, eventually, at $T^{\infty} = T_{cn}^{\infty}(0) \approx 2 \times 10^8$ K it penetrates the stellar centre.

4 OSCILLATION SPECTRA AND MODES

Figure 2 presents normalized eigenfrequencies ω_{ln} (in units of $\tilde{\omega} = c/R \approx 2.5 \times 10^4$ s $^{-1}$) versus internal temperature T^{∞} for SFL oscillations of multipolarity $l = 0, 1, 2$, and 3 . For each l we plot a set of oscillation modes that differ by the number of radial nodes $n = 0$ (solid lines), $n = 1$ (dots), $n = 2$ (long dashes), $n = 3$ (long-short dashes), and $n = 4$ (dashes). One sees that the higher the n the larger the ω_{ln} . By the hatches in the bottom panel of the figure we show the SFL-region; as expected, the size of this region depends on T^{∞} . The grey-shaded area corresponds to the crust and a region in the core where all neutrons are unpaired. A similar shaded area on the four upper panels shows temperatures $T^{\infty} \geq \mathfrak{T}_{cn}^{\infty}$ for which *all* neutron matter in the core is normal. In the latter case there are no SFL modes in NS.

Before further discussing spectra in Fig. 2 it is convenient to describe briefly Fig. 3 that presents eigenfunctions $\delta\mu_{ln}(r)$ normalized to unity in the maximum. The solid lines correspond to radial oscillation modes ($l = 0$), dotted and dashed lines describe dipole ($l = 1$) and quadrupole ($l = 2$) modes, respectively. Each column in the figure contains four panels which are plotted for the following temperatures (from bottom to the top): $T^{\infty} = 10^8, 2 \times 10^8, 3 \times 10^8$, and 4×10^8 K. For any of these temperatures we have five panels in a row, which correspond to (from left to right) $n = 0, 1, 2, 3$, and 4 radial nodes of $\delta\mu_{ln}(r)$. The stellar regions where neutrons are normal, are shaded in Fig. 3.

At $T^{\infty} \lesssim \mathfrak{T}_{cn}^{\infty}$ the size of SFL-region rapidly increases

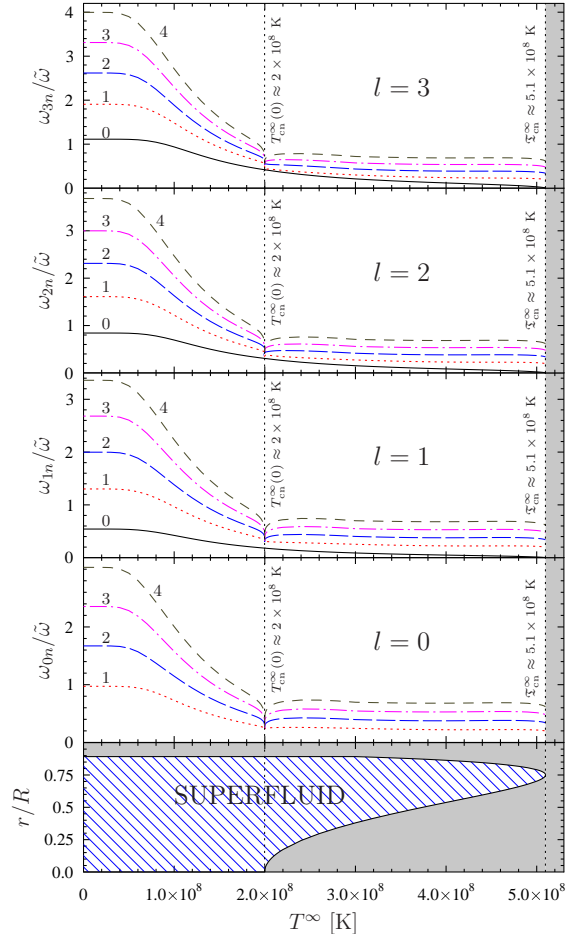


Figure 2. (color online) Eigenfrequencies ω_{ln} versus T^{∞} for multiplicities $l = 0, 1, 2$, and 3 . For each l a set of curves is plotted with $n = 0, 1, 2, 3$ or 4 . At $T^{\infty} \leq T_{cn}^{\infty}(0) \approx 2 \times 10^8$ K (see the vertical short-dashed line) superfluidity occupies the stellar centre. The bottom panel shows variation of SFL-region with T^{∞} . For more details see the text.

as the star cools down, whereas the eigenfrequencies are almost temperature-independent for $T^{\infty} \gtrsim 3 \times 10^8$ K (except for the modes with $n = 0$, see Fig. 2 and discussion below). This is so because of compensation of two opposite tendencies: (i) expansion of the SFL-region and (ii) increasing of the local speed of SFL sound $v^{\text{sf}} = e^{-\nu/4} \sqrt{-h} \mathfrak{B}$ with decreasing T^{∞} (see Gusakov & Andersson 2006 for details on v^{sf}). The tendency (i) leads to decreasing while (ii) leads to growing of the eigenfrequencies ω_{ln} .

The qualitative behaviour of ω_{ln} and $\delta\mu_{ln}(r)$ at 3×10^8 K $\lesssim T^{\infty} \lesssim \mathfrak{T}_{cn}^{\infty}$ follows from simple arguments. The parameter h is small there, so that it is sufficient to retain only the terms $\propto h^{-1}$ in Eq. (5). As a result, for $T^{\infty} \gtrsim 3 \times 10^8$ K $\delta\mu_{ln}(r)$ will be almost independent of l (see Fig. 3). Furthermore, at $T^{\infty} \gtrsim 4 \times 10^8$ K the function h can be approximated as $h \approx A [(\mathfrak{T}_{cn}^{\infty} - T^{\infty}) - B(r - r_{cn}^{\max})^2]$, where A and B are some constants depending on a NS model. Using this approximation, one can analytically solve Eq. (5) and find that eigenfunctions $\delta\mu_{ln}(r)$ are proportional to the Legendre polynomials P_n while the eigenfrequencies $\omega_{ln} \propto \sqrt{n(n+1)}$ and are independent of T^{∞} (see Figs. 2 and 3 for $T^{\infty} \gtrsim 4 \times 10^8$ K). For the modes with $n = 0$

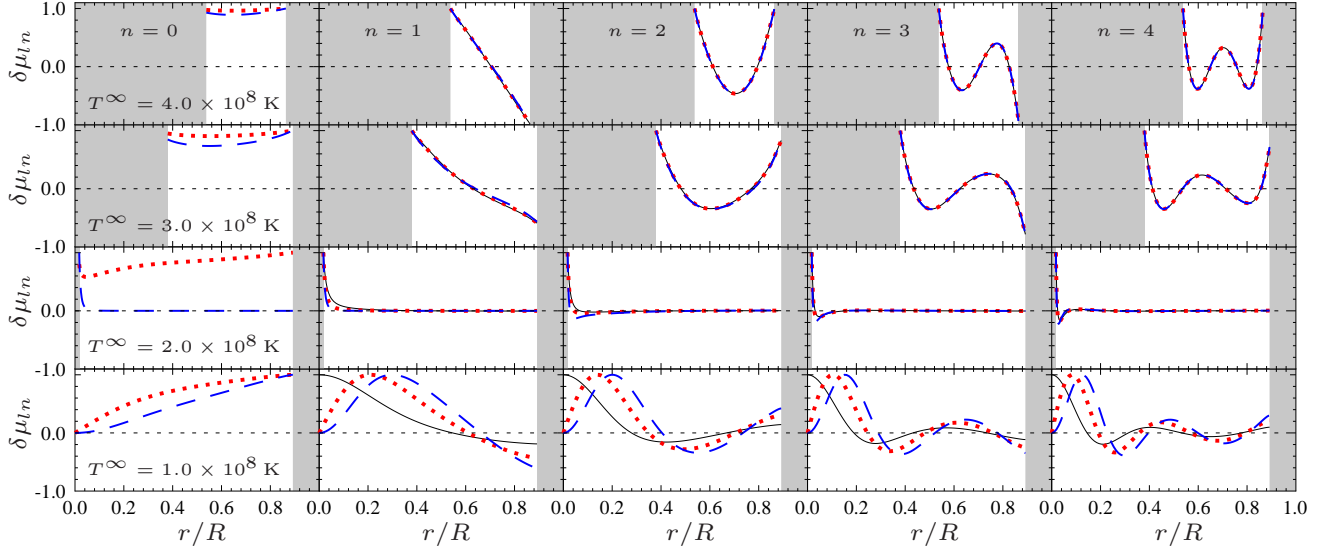


Figure 3. (color online) Eigenfunctions $\delta\mu_n$ versus r for $T^\infty = 10^8, 2 \times 10^8, 3 \times 10^8,$ and 4×10^8 K (5 panels in a row for each temperature). The columns of panels are for $n = 0, 1, 2, 3,$ and 4 radial nodes. Solid, dotted, and dashed lines correspond to multipoles $l = 0, 1,$ and $2,$ respectively. For more details see the text.

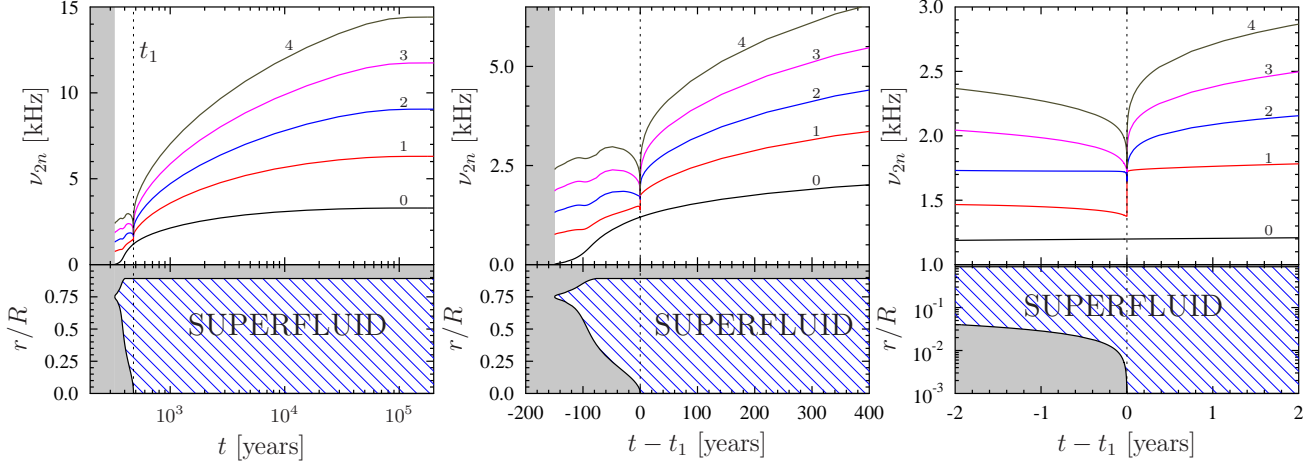


Figure 4. (color online) Upper panels: The oscillation frequencies ν_{2n} of quadrupole modes with $n = 0, \dots, 4$ versus stellar age t . Vertical dashed lines show the stellar age t_1 at which neutron superfluidity first appears in the stellar centre. Bottom panels: Variation of SFL-region with t . For more details see the text and captions to Figs. 2 and 3.

this estimate gives $\omega_{10} = 0$. As follows from Fig. 2, in that case the eigenfrequencies are indeed small but nonzero. To improve the estimate for ω_{10} one should take into account the term depending on $l(l+1)/r^2$ in Eq. (5). Because at $T^\infty \gtrsim 4 \times 10^8$ K $\delta\mu_{10}(r)$ is almost constant (see top-left panel in Fig. 3), one can put $\delta\mu'_{10} \approx 0$ and $\delta\mu''_{10} \approx 0$. Using then Eq. (5), one obtains the following estimate for ω_{10} : $\omega_{10} \propto \sqrt{l(l+1)} v^{\text{sf}}/r_{\text{cn}}^{\text{max}} \propto \sqrt{l(l+1)} \sqrt{1 - T^\infty/\mathfrak{T}_{\text{cn}}^\infty}$. This formula indicates that ω_{10} depends only on $T^\infty/\mathfrak{T}_{\text{cn}}^\infty$ (but not on the size of SFL-region) and vanishes at $T^\infty = \mathfrak{T}_{\text{cn}}^\infty$ (see Fig. 2). It remains to note that for $l = 0$ Eq. (5) has a static solution $\delta\mu_{00} = \delta\mu^\infty = \text{const}$ and $\omega_{00} = 0$, which describes a star in hydrostatic and diffusive equilibrium (but not necessarily in beta-equilibrium, see Gusakov & Andersson 2006 for more details). It should also be stressed that approximate formulas for eigenfrequencies found above is not a special

feature of our microphysical model. Rather, it is inherent in *all* NSs for which the maximum of $T_{\text{cn}}^\infty(r)$ lies between the centre and the crust-core boundary.

At T^∞ slightly exceeding $T_{\text{cn}}^\infty(0)$ the size of SFL-region rapidly expands to the stellar centre as the star cools down. The reason for that is weak dependence of T_{cn}^∞ on r at $r \lesssim 0.1 R$ (see the right panel of Fig. 1). Since $T^\infty \approx T_{\text{cn}}^\infty$ for $r \lesssim 0.1 R$, v^{sf} is close to 0 there. This results in a noticeable decrease of ω_{ln} with $n \geq 1$ near $T_{\text{cn}}^\infty(0)$ (see Fig. 2). In particular, at $T^\infty = 2 \times 10^8$ K the corresponding oscillation modes are all localized in the vicinity of the stellar centre, where v^{sf} is small (see Fig. 3). During subsequent cooling [for $T^\infty \lesssim T_{\text{cn}}^\infty(0)$] the entire core is already occupied by the neutron superfluidity and increasing of v^{sf} , especially in the central regions of the star, leads to growing of ω_{ln} . When T^∞ drops below $\sim 4 \times 10^7$ K the eigenfrequencies ω_{ln} and

eigenfunctions $\delta\mu_{ln}(r)$ become almost independent of T^∞ , since h (and v^{sf}) approach their asymptotes at $T^\infty = 0$.

Let us now discuss the temporal evolution of oscillation spectra during the star cooling. To simulate cooling we apply a slightly updated version of the code discussed by Gusakov et al. (2005). The onset of neutron superfluidity is accompanied by an abrupt acceleration of cooling due to the Cooper pairing neutrino emission process (see Shternin et al. 2011 for recent observational evidences of such cooling). As is demonstrated in Fig. 4, this process leads to a rapid evolution of oscillation spectrum. Upper panels in Fig. 4 show the eigenfrequencies $\nu_{2n} \equiv \omega_{2n}/(2\pi)$ of quadrupole modes ($n = 0, \dots, 4$) versus NS age t . The lower panels illustrate change of the SFL-region with t . On the left upper panel the functions $\nu_{2n}(t)$ are plotted for the time interval from 200 to 2×10^5 years. After the onset of neutron superfluidity (at $t \approx 330$ years) the oscillation spectrum rapidly changes and approaches its zero-temperature asymptote only at $t \gtrsim 10^5$ years. At the star age $t_1 \approx 480$ years superfluidity penetrate the stellar centre [this corresponds to $T^\infty = T_{\text{cn}}^\infty(0)$]. The period of time $|t - t_1| \ll t_1$ is accompanied by a very fast evolution of the spectrum. In more detail the evolution is shown in the central panels which span an interval of approximately 600 years of NS cooling. The time t in these panels is counted from t_1 . The right panels in Fig. 4 show the only four-year episode of NS life in the vicinity of t_1 . One sees that even for such a small period of time the frequencies of some oscillation modes increase by more than 10%, whereas the frequency of the mode with four radial nodes changes noticeably on a time-scale of a few months (!).

5 SUMMARY AND OUTLOOK

In this letter we study, for the first time, nonradial oscillations of SFL NSs at finite temperatures. Use of an approach developed in GK11 enable us to solve this problem in full general relativity, employing the realistic equation of state (APR) and realistic, density-dependent profiles of nucleon critical temperatures (Fig. 1). It is shown that equations describing SFL modes can generally be reduced to the simple second-order differential Eq. (5). The eigenfrequency spectrum (Fig. 2) and eigenfunctions (Fig. 3) for this equation are carefully analysed. It is demonstrated that dependence of eigenfrequencies ω_{ln} on T^∞ is determined by two competing effects: (i) decreasing of ω_{ln} with expanding SFL-region and (ii) growing of ω_{ln} with increasing of the local speed of SFL sound v^{sf} . These results agree with the conclusions made by Kantor and Gusakov (2011) for a radially oscillating NS.

In addition, we examine the evolution of oscillation spectrum in the course of NS cooling (Fig. 4). We find that acceleration of NS cooling soon after the onset of triplet neutron superfluidity leads to a very fast modification of the spectrum – the eigenfrequencies can vary dramatically on a time-scale of months.

In the present work we completely ignore various dissipative effects in pulsating SFL NSs. Meanwhile, our results provide a strong basis to study these effects using the perturbative scheme suggested in GK11. In particular, to determine the damping time τ of some normal or SFL mode one could proceed in the following steps: (i) find the vec-

tors u^μ and $w_{(n)}^\mu$ assuming $s = 0$ and neglecting dissipation (see GK11 and Sec. 2); (ii) use them to calculate the dissipative terms entering the SFL hydrodynamics (and hence the rate of change \dot{E} of the oscillation energy E , see, e.g., Kantor & Gusakov 2011); (iii) calculate τ as $\tau = -E/(\dot{E})$.

The other important problem concerns gravitational radiation from pulsating SFL NSs. The radiation from normal modes can be accurately calculated already in the $s = 0$ limit (and will be the same as that for a nonsuperfluid NS). In turn, SFL modes are not coupled with the metric in the $s = 0$ limit, so that to calculate gravitational radiation from them one must use the first-order perturbation theory in s . Interestingly, this problem is equivalent to finding gravitational radiation from a *normal* NS experiencing oscillations under an action of a small external force $\propto s$. An intensity of such radiation will be reduced by a factor of $s^2 \sim 10^{-3}$ in comparison to normal modes with the same E . Detailed studies of dissipation in SFL NSs are a very important task, e.g., for calculation of the instability windows of r-modes; we plan to address it in the near future.

ACKNOWLEDGMENTS

The authors are grateful to E.M. Kantor, D.G. Yakovlev, and A.V. Brillante for useful comments. This work was partially supported by RFBR (grant 11-02-00253-a), by RF president program (grants NSh-3769.2010.2 and MK-5857.2010.2), and by the Dynasty foundation.

REFERENCES

- Akmal A., Pandharipande V.R., Ravenhall D.G., 1998, Phys. Rev. C, 58, 1804
- Andersson N., Comer G.L., Langlois D., 2002, Phys. Rev. D, 66, 104002
- Andersson N., Ferrari V., Jones D.I., Kokkotas K.D., Krishnan B., Read J.S., Rezzolla L., Zink B., 2011, Gen. Rel. Grav. 43, 409
- Benhar O., Ferrari V., Gualtieri L., 2004, Phys. Rev. D, 70, 124015
- Comer G.L., Langlois D., Lin L.-M., 1999, Phys. Rev. D, 60, 104025
- Gnedin O.Y., Yakovlev D.G., Potekhin, A.Y., 2001, MNRAS, 324, 725
- Gusakov M.E., 2007, Phys. Rev. D, 76, 083001
- Gusakov M.E., Andersson N., 2006, MNRAS, 372, 1776
- Gusakov M.E., Kantor E.M., 2011, Phys. Rev. D, 83, 081304 (R)
- Gusakov M.E., Kaminker A.D., Yakovlev D.G., Gnedin O.Y., 2005, MNRAS, 363, 555
- Haskell B., Andersson N., 2010, MNRAS, 408, 1897
- Haskell B., Andersson N., Passamonti A., 2009, MNRAS, 397, 1464
- Kantor E.M., Gusakov M.E., 2011, Phys. Rev. D, 83, 103008
- Lin L.-M., Andersson N., Comer G.L., 2008, Phys. Rev. D, 78, 083008
- Lindblom L., Mendel G., 1994, ApJ, 421, 689
- Lombardo U., Schulze H.-J., 2001, Lect. Notes Phys. 578, 30

- McDermott P.N., Van Horn H.M., Hansen C.J., 1988, ApJ, 325, 725
Shternin P.S., Yakovlev D.G., Heinke C.O., Ho W.C.G., Patnaude D.J., 2011, MNRAS, 412, L108
Thorne K.S., Campolattaro A., 1967, ApJ, 49, 591
Yoshida S., Lee U., 2003, Phys. Rev. D, 67, 124019